Periodic Optimal Trajectories with Singular Control for Aircraft with High Aerodynamic Efficiency

Prof. Dr.-Ing. Gottfried Sachs
Dipl.-Ing. Klaus Lesch

Prof. Dr. Hans Georg Bock
Dipl.-Math. Marc Steinbach

Abstract. Fuel minimum range cruise of aircraft with high aerodynamic efficiency is considered as an optimal periodic control problem. Optimality conditions for trajectories with singular arcs and state variable constraints are derived.

Computation of periodic optimal trajectories in the case addressed presents strong requirements on the numerical algorithm. Computational difficulties become larger when aerodynamic efficiency is increased and wing loading is decreased. The specific nature of the numerical problems encountered and the means used to overcome them are described.

1. Nomenclature

C_{D}	drag coefficient
C_{L}	lift coefficient
C_{L}^{*}	lift coefficient at maximum lift/drag ratio
c	normalized period length
D	drag
E	aerodynamic efficiency, $E = (C_{\mathrm{L}}/C_{\mathrm{D}})_{\max}$
g	acceleration due to gravity
H	Hamiltonian
h	altitude
J	performance criterion
K	factor according to lift dependent drag, $C_{\mathrm{D}} = C_{\mathrm{D}_0} + KC_{\mathrm{L}}^2$
L	lift
m	mass
m_{V}	exponent denoting the effect of speed on fuel consumption
P	propulsive power, $P = TV$

S	reference area
$\overline{S}$	switching function
T	thrust
V	speed
V_0^*	speed for best glide ratio at sea level ($h = 0$)
x	horizontal coordinate
y	state variable vector
γ	flight path angle
δ	throttle setting
ε	glide ratio
λ	Lagrange multiplier
ϱ	atmospheric density
σ	fuel consumption factor
ξ	independent variable
$\overline{}$	a bar denotes a normalized quantity, e.g. $\overline{V}$

2. Introduction

The cruise of aircraft for maximizing range classically consists of a steady-state flight at constant speed and/or altitude with a basically straight trajectory. The control and state variables are chosen such that the fuel consumption is minimized. However, it has been shown that this type of cruise is not generally optimal, and results have been presented for optimal aircraft cruise which shows a periodic behavior (Refs. 1-10). The trajectory of such a cruise basically consists of periodically repeated cycles each of which shows a climb followed by a descent, with thrust alternately operated at high and low throttle settings.

In some cases, periodic optimal cruise shows singular arcs. This means that the throttle setting takes on intermediate values between the maximum and minimum bounds during a non-zero portion of the flight time. It has been shown that the dependence of thrust specific fuel consumption on speed has a significant effect as regards the existence of singular arcs (Refs. 9, 10).

It is the purpose of this paper to provide more insight into periodic optimal cruise of aircraft with singular arcs. Emphasis is placed on aircraft with high aerodynamic efficiency like modern motorgliders. Accordingly, the computational difficulties which exist in determining periodic optimal trajectories for such aircraft are of particular interest. Special numerical techniques are applied concerning the formulation of the multipoint boundary value problem and the solution of the linearized system in the iterative procedure used.

3. Problem Formulation

The optimal control problem consists of minimizing the fuel consumption per range of aircraft. This can be formulated by introducing the performance criterion

$$J = \frac{m_f(x_{\rm cyc})}{x_{\rm cyc}} \tag{1}$$

where m_f is the consumed fuel and x_{cyc} is the (horizontal) length of one period of the trajectory. A period may be considered as a basic element of the whole trajectory.

The performance criterion is subject to the equations of motion. For a non-dimensional form, the following normalization is introduced:

$$\begin{aligned} \overline{V} &= \frac{V}{V_0^*}\,, \quad \overline{h} = \frac{hg}{V_0^{*2}}\,, \quad \overline{m}_{\mathrm{f}} = \frac{m_{\mathrm{f}}}{m}\,, \quad \xi = \frac{x}{x_{\mathrm{cyc}}}\,, \quad c = \frac{x_{\mathrm{cyc}}g}{V_0^{*2}} \\ \overline{C}_{\mathrm{L}} &= \frac{C_{\mathrm{L}}}{C_{\mathrm{L}}^*}\,, \quad \overline{C}_{\mathrm{D}} = \frac{C_{\mathrm{D}}}{C_{\mathrm{L}}^*}\,, \quad \overline{T} = \frac{T}{mg}\,, \quad \overline{J} = \frac{\overline{m}_{\mathrm{f}}}{c} \end{aligned} \tag{2}$$

Consequently, the equations of motion may be written as

$$\begin{aligned} \frac{\mathrm{d}\overline{V}}{\mathrm{d}\xi} &= c\frac{1}{\overline{V}}\left[\frac{\overline{T}(\overline{V},\overline{h};\delta) - \overline{\varrho}\overline{V}^2\overline{C}_{\mathrm{D}}}{\cos\gamma} - \tan\gamma\right] \\ \frac{\mathrm{d}\gamma}{\mathrm{d}\xi} &= c\left[\frac{\overline{\varrho}\overline{C}_{\mathrm{L}}}{\cos\gamma} - \frac{1}{\overline{V}^2}\right] \\ \frac{\mathrm{d}\overline{h}}{\mathrm{d}\xi} &= c\tan\gamma \\ \frac{\mathrm{d}\overline{m}_f}{\mathrm{d}\xi} &= c\frac{V_0^*}{g}\frac{\dot{\overline{m}}_{\mathrm{f}}}{\overline{V}\cos\gamma} \end{aligned} \tag{3}$$

The aerodynamic drag polar is modelled as

$$\overline{C}_{\mathrm{D}} = \frac{\varepsilon_{\mathrm{min}}}{2}(1 + \overline{C}_{\mathrm{L}}^2) \tag{4}$$

The thrust model accounts for the effect of speed, altitude and throttle setting. It may be expressed as

$$\overline{T}(\overline{V},\overline{h};\delta) = \delta\,\overline{T}_{\mathrm{max}}(\overline{V},\overline{h}) \tag{5}$$

Fuel consumption characteristics are described by the relation

$$\dot{\overline{m}}_{\mathrm{f}} = \dot{\overline{m}}_{\mathrm{f}0}(\overline{h}) + \delta\, g\, \sigma(\overline{V})\,\overline{T}_{\mathrm{max}}(\overline{V},\overline{h}) \tag{6}$$

The mass of the aircraft can be considered constant for one period, since the fuel consumed during such a time interval is small as compared with the total mass, i.e.,

$$\overline{m}_{\mathrm{f}}(1) - \overline{m}_{\mathrm{f}}(0) \ll 1 \tag{7}$$

Periodicity of the flight path implies the boundary conditions

$$\overline{V}(0) = \overline{V}(1)\,, \qquad \gamma(0) = \gamma(1)\,, \qquad \overline{h}(0) = \overline{h}(1) \tag{8a}$$

The initial condition for the fuel mass can be written as

$$\overline{m}_{\mathrm{f}}(0) = 0 \tag{8b}$$

Control variables are the lift coefficient $\overline{C}_{\mathrm{L}}$ and the throttle setting δ which are subject to the inequality constraints

$$\overline{C}_{\mathrm{L_{min}}} \leq \overline{C}_{\mathrm{L}} \leq \overline{C}_{\mathrm{L_{max}}} , \qquad 0 \leq \delta \leq 1 \tag{9}$$

The atmospheric model which is used for describing air density and thrust dependence on altitude agrees with the ICAO Standard Atmosphere (Ref. 11).

The periodic control problem is to find the control histories $\overline{C}_{\mathrm{L}}$ and δ, the initial states $(\overline{V}(0),\ \gamma(0),\ \overline{h}(0))$ and the periodic cycle length c which minimize the performance criterion $\overline{J} = \overline{m}_{\mathrm{f}}(1)/c$ subject to the dynamic system Eq. (3), the boundary conditions Eqs. (8a, b), and the inequality constraints for the control variables Eq. (9).

4. Conditions for Optimality and Singular Control

Necessary conditions for optimality can be determined by applying the minimum principle. For this purpose, the Hamiltonian is defined as

$$H = \lambda_{\mathrm{V}} \frac{\mathrm{d}\overline{V}}{\mathrm{d}\xi} + \lambda_{\gamma} \frac{\mathrm{d}\gamma}{\mathrm{d}\xi} + \lambda_{\mathrm{h}} \frac{\mathrm{d}\overline{h}}{\mathrm{d}\xi} + \lambda_{\mathrm{f}} \frac{\mathrm{d}\overline{m}_{\mathrm{f}}}{\mathrm{d}\xi} , \tag{10}$$

where the Lagrange multipliers $\lambda = (\lambda_{\mathrm{V}}, \lambda_{\gamma}, \lambda_{\mathrm{h}}, \lambda_{\mathrm{f}})^T$ have been adjoined to the dynamic system of Eq. (3). The Lagrange multipliers are determined by

$$\frac{\mathrm{d}\lambda_{\mathrm{V}}}{\mathrm{d}\xi} = -\frac{\partial H}{\partial \overline{V}} , \quad \frac{\mathrm{d}\lambda_{\gamma}}{\mathrm{d}\xi} = -\frac{\partial H}{\partial \gamma} , \quad \frac{\mathrm{d}\lambda_{\mathrm{h}}}{\mathrm{d}\xi} = -\frac{\partial H}{\partial \overline{h}} , \quad \frac{\mathrm{d}\lambda_{\mathrm{f}}}{\mathrm{d}\xi} = 0 , \tag{11}$$

with boundary conditions

$$\lambda_{\mathrm{V}}(0) = \lambda_{\mathrm{V}}(1) , \ \lambda_{\gamma}(0) = \lambda_{\gamma}(1) , \ \lambda_{\mathrm{h}}(0) = \lambda_{\mathrm{h}}(1) , \ \lambda_{\mathrm{f}}(1) = 1/c \tag{12}$$

The optimal controls $\overline{C}_{\mathrm{L}}$ and δ are such that H is minimized pointwise along the optimal trajectory. For this reason, $\overline{C}_{\mathrm{L}}$ is determined either by

$$\partial H / \partial \overline{C}_{\mathrm{L}} = 0 \tag{13}$$

or by the constraining bounds of Eq. (9).

With regard to throttle setting, H is linear in δ. Therefore, a bang-bang type of control and/or singular arcs can exist. Evaluation of the switching function

$$\overline{S}(y,\ \lambda) = \frac{\partial}{\partial \delta} H(y,\ \lambda;\ \overline{C}_{\mathrm{L}},\ \delta) \tag{14}$$

leads to

$$\begin{aligned} \delta &= 0 \quad \text{if} \quad \overline{S}(y,\ \lambda) > 0 , \\ \delta &= 1 \quad \text{if} \quad \overline{S}(y,\ \lambda) < 0 , \\ \delta &: \text{singular} \quad \text{if} \quad \overline{S}(y,\ \lambda) = 0 \text{ on a finite interval of } \xi , \end{aligned} \tag{15}$$

where $y = (\overline{V},\ \gamma,\ \overline{h},\ \overline{m}_{\mathrm{f}})^T$.

The order of the singular arc is $p = 1$, because

$$\frac{\partial}{\partial \delta} \overline{S}^{(1)} = 0 \,, \quad \frac{\partial}{\partial \delta} \overline{S}^{(2)} \neq 0 \tag{16}$$

where

$$\overline{S}^{(i)}(y,\, \lambda;\, \overline{C}_{\mathrm{L}},\, \delta) = \frac{d^i}{\mathrm{d}\xi^i} \overline{S}(y,\, \lambda;\, \overline{C}_{\mathrm{L}}), \quad i = 1,\, 2 \tag{17}$$

The relation $\overline{S}^{(2)}(y,\, \lambda;\, \overline{C}_{\mathrm{L}},\, \delta) = 0$ can be used to find the singular control

$$\delta = \delta_{\mathrm{sing}}(y,\, \lambda;\, \overline{C}_{\mathrm{L}}) \tag{18}$$

The switching structure of the optimal control is considered to be known, and the conditions described above have to be checked and evaluated along the trajectory.

The system described by Eq. (3) is autonomous, so that the Hamiltonian H is constant. Since furthermore the cycle lenght c is considered free, the following relation holds:

$$H = \frac{\overline{m}_{\mathrm{f}}(1)}{c} \tag{19}$$

5. Further Considerations

Additional conditions exist for constraint arcs where the altitude range is limited. This concerns a minimum admissible altitude and, in some cases, an additional maximum altitude limit

$$G_1(\overline{h}) = -\overline{h} \leq 0 \,, \qquad G_2(\overline{h}) = \overline{h} - \overline{h}_{\mathrm{max}} \leq 0 \tag{20}$$

The conditions for dealing with the constraints are formulated according to Ref. 13.

There are additional necessary optimality conditions which have been evaluated in the investigation. They may be briefly addressed as

a) Legendre Clebsch condition (Ref. 12), (21)

b) Kelley condition (Ref. 12), (22)

c) Goh condition (Ref. 12), (23)

d) Robbins equality condition (Ref. 12). (24)

6. Periodic Optimum Trajectories with Singular Control

As an illustration for the type of trajectories of interest, some examples are considered first. They are presented in Figs. 1-3.

In Fig. 1, state and control variables of optimal trajectories for minimum fuel consumption per range are shown. A periodic optimal trajectory can be characterized as consisting of a climbing flight phase at maximum thrust setting followed by a sinking phase at zero thrust. The singular thrust arcs may be considered as elements connecting these phases. The throttle control shows a pronounced singular behavior for both transitions during which it changes from one boundary value to the other. The lift coefficient which is the other control appears to be activated primarily during the singular arcs.

The trajectory belonging to a low aerodynamic efficiency shows changes more gradual. By increasing aerodynamic efficiency, the relative length of the singular arcs decreases. Accordingly, the slopes of the singular thrust arcs become steeper and the lift coefficient shows less changes.

More insight into the behavior of the singular arcs is presented in Figs. 2 and 3 which show the switching functions and their derivatives for the cases considered in Fig. 1. As may be seen, similar characteristics develop when changing the aerodynamic efficiency from a low to a high value. This particularly concerns the slopes of the functions in the neighbouring regions of the singular arcs. A pronounced example is presented in the lowest part of Fig. 3 which shows a peak type behavior of a function which, in fact, is smooth.

7. Numerical Problems and Improvements

The examples presented in Figs. 1-3 provide an indication of the numerical problems which exist when aerodynamic efficiency is increased. Another effect which produces numerical difficulties is due to a decrease of wing loading m/S. This is illustrated in Fig. 4 which shows homotopy paths concerning solutions when changing both factors addressed, with $V_0^* = \sqrt{m/S}\sqrt{2g/(C_{\mathrm{L}}^* \varrho_0)}$ used as a measure for wing loading. The break-down points due to a convergence failure are indicated. They concern an increase of aerodynamic efficiency as well as a decrease of wing loading.

An improvement is possible by normalizing state and adjoint variables such that they are of about equal magnitude. Another measure applied for improving convergence is a different time scaling of each shooting interval. In addition, an alternative formulation of the singular control and the switching conditions can be applied where the adjoint variables λ_{V} and λ_γ are eliminated. With this formulation, it is possible to stay on the singular surface during the integration. The standard formulation where λ_{V} and λ_γ are not eliminated leaves the singular surface during integration because of the numerical deficiencies concerning $\overline{S} = 0$ and $\overline{S}^{(1)} = 0$. A final measure which may be applied concerns a refinement of the multiple shooting grid up to 60 nodes.

With the measures described a homotopy continuation could be achieved. This was applied to a homotopy path showing a combination of aerodynamic efficiency and wing loading as indicated in Fig. 4. A convergence failure again occured before regions of interest for aerodynamic efficiency and wing loading were reached.

In order to find out more about the nature of the difficulties, the last solution that could be obtained before the homotopy break-down was analyzed. A new generalized version of the Multiple Shooting code PARFIT (Ref. 14) was applied for a detailed investigation of the numerical multi-point boundary value problem (MPBVP). Even though this code can handle over- and underdetermined systems (see below), the numerical MPBVP was always formulated as a regular (nonlinear) system with fixed "phase" of the periodic trajectory. In the following part, the results of our analysis are summarized and the strategy used for overcoming the difficulties is outlined.

1) The norms of the sensitivity matrices on the shooting intervals $I_j = [\tau_j, \tau_{j+1}]$,

$$G_j = \frac{\partial}{\partial s_j} z(\tau_{j+1}; \tau_j, s_j), \qquad z(\tau_j; \tau_j, s_j) = s_j \tag{25}$$

are extremely large. Fig. 5 shows the error propagation factors

$$\gamma_j = \|G_j\|_\infty = \max_i \left\{ \sum_k |(G_j)_{ik}| \right\}, \tag{26}$$

which indicate that an initial error δs_j at τ_j may be blown up to a magnitude $\gamma_j \|\delta s_j\|_\infty$ at τ_{j+1}. In other words, $\kappa_j = \log_{10} \gamma_j$ decimal digits are lost during numerical integration on I_j. Obviously, the differential equations are very unstable.

The instability does not only influence the computation of the Newton step in each iteration, there is also an important side effect. All the interior point conditions are not taken at shooting nodes. Hence, the computation of the corresponding derivative matrices

$$D_j = \frac{\partial}{\partial s_j} r\left(z(0), \ldots, z(1)\right), \qquad z(\xi) = z(\xi; \tau_j, s_j) \text{ on } I_j \tag{27}$$

involves multiplication by certain transition matrices. Thus, they are also large and loss of decimals at fractions of subintervals decreases their accuracy.

2) The minimum principle approach may always cause stability problems to some extent because of the symplectic structure of the canonical system. But even with unstable differential equations the MPBVP may be well-posed, provided there is some dichotomy and the boundary conditions are well-posed. The latter point was investigated in more detail using sophisticated linear algebra methods. A condensing algorithm of Ref. 14 was used to generate an orthonormal base for the linearized problem such that the solution space of the matching conditions and the solution space of the multi-point boundary conditions are spanned as orthogonal complements. This allows elimination of the variables representing the discretization of the ordinary differential equations system in an optimal manner, i.e., in a way that corresponds to the dichotomy properties of the differential equations. Therefore the condition number of the special condensed system generated this way describes the actual well-posedness of the boundary conditions.

The condition number of the condensed system was found to be extremely large with very small singular values present; estimates are shown in Fig. 6. Hence, the multi-point boundary conditions were in fact ill-posed. As a consequence, no reliable Newton increments could be obtained as solution of the linearized system. This turned out to be the most serious problem at the break-down point of the homotopy.

To overcome the difficulties, the round-off errors had to be reduced and the MPBVP had to be reformulated. In the following, the techniques used successfully to achieve these goals are briefly described.

1a) The error propagation factors on the intervals are drastically reduced by refining the mesh. (Taking a fraction α of subinterval I_j approximately reduces γ_j to γ_j^α.) It may be noted that refining the mesh improves the numerical behavior only as long as the reduction in γ_j is not counter-balanced by increasing roundoff errors in linear algebra operations.

During continuation of the homotopy, error propagation became the dominant difficulty, and the mesh was subsequently refined using 32, 64, 96 and 192 subintervals. Along with this, the distribution of the nodes was adapted to the local stability properties.

1b) Conventional (external) numerical differentiation approximates the transition matrices with low accuracy because of nonlinear coupling and instability. To get more accurate derivative matrices, the "Internal Numerical Differentiation" technique described in Ref. 14 was applied. In the most difficult cases it was still necessary to use the highest available integration accuracy (error per step $\leq 10^{-13}$). The CPU time spent for integrating and generating derivative matrices was in the range of 90 to 99.5% of the total CPU time required by PARFIT.

2) To reduce the condition number, the MPBVP was reformulated as described in the next section, and stable linear algebra methods were applied. After condensing the system by the aforementioned special algorithm, the condensed system is treated by a stable solver for constrained least-squares problems, which is capable of solving over- and underdetermined problems and includes pivoting and a rank and condition analysis. The combination of both algorithms provides a powerful tool not only for analyzing the MPBVP but also for developing an appropriate numerical formulation, thus leading to considerable insight.

The crucial point in solving a difficult optimal control problem is the numerical formulation of the associated MPBVP. Usually several equivalent formulations exist leading to more or less well-posed boundary conditions.

Since the precise switching structure is considered to be known in the problem dealt with, a "variable mesh" technique as described in Ref. 13 was applied. Thus placing the switching points on shooting nodes reduces round-off errors and makes the numerical MPBVP more stable. This technique also prevents switching points from traversing nodes during iteration, a very important advantage especially for fine meshes.

After choosing this problem transformation still a large number of equivalent sets of necessary conditions exist, especially as regards the choice of entry and exit conditions of singular arcs. The periodicity of the autonomous control problem adds an additional "phase shift" degree of freedom, hence the set of necessary conditions derived by applying the minimum principle is degenerate. Since switch and jump conditions must be satisfied, the phase should be fixed, and the singularity calls for a normalization condition. (Alternatively, one could simply solve the singular system using a pseudo-inverse, at least in the absence of discontinuities.)

In our problem physical knowledge and mathematical experience were used to choose an appropriate numerical MPBVP. It should be pointed out, however, that any number of necessary conditions could be included in the MPBVP (in a least-squares sense), and the linear solver would automatically pick an appropriate combination by its pivoting algorithm. This allows for an easy and safe treatment of the problem without investigating the details of its nature.

8. Fuel Savings

An evaluation concerning the reduction of fuel consumption per range is presented in Fig. 7 which shows a comparison between periodic optimal cruise and the best steady-state cruise. The result is that the gain due to periodic optimal control is comparatively small. The gains are reduced when aerodynamic efficiency is increased and maximum engine power available is decreased.

The fuel consumption model used for the results presented in Fig. 7 shows a linear dependence on throttle setting, with zero fuel flow at idling ($\bar{\dot{m}}_{f_0} = 0$). This model may be considered as an idealized characteristic. A model more realistic accounts for a non-zero fuel consumption at idling $\bar{\dot{m}}_{f_0} \neq 0$. This is illustrated in Fig. 8 which shows both models addressed. For the more realistic model, the gains achievable with optimal periodic cruise can reach a level of practical significance when the engine is switched off during phases for which $\delta = 0$ is required by the optimality conditions and when the maximum altitude is constrained such as for aircraft with non-pressurized cabins (Ref. 15). An evaluation is presented in Fig. 9 which provides a quantitative insight into the gains achievable for a wide range of relevant aircraft performance parameters (Ref. 9).

9. Conclusions

For minimizing fuel consumption in aircraft range cruise, it is shown that periodic optimal trajectory solutions with singular control exist. Singular arcs are favored when thrust specific fuel consumption is linearly dependent on speed. Such a characteristic is of practical significance because it is existent with propeller driven aircraft.

The improvements due to periodic optimal control are also considered. For a wide range of relevant aircraft performance parameters, it is shown which are the reductions in fuel consumption as compared with the best steady-state cruise. The improvements appear to be comparatively small when an idealized fuel consumption model is considered. There may be a significant improvement for a more realistic model accounting for a non-zero fuel flow at idling.

To generate optimal trajectories when changing aerodynamic efficiency and wing loading, a homotopy technique is used. In the progress of the homotopy, convergence problems result when aerodynamic efficiency is increased and wing loading is decreased. To reach a domain valid for modern motorgliders, special numerical improvements are required. After analyzing the problem, reasons for the numerical difficulties were found in extremely large sensitivity matrices on the shooting intervals and very ill-posed multipoint boundary conditions. Successful measures to decrease the sensitivity matrices are the refinement of the multiple shooting mesh and the use of the "Internal Numerical Differentiation" technique together with a very high integration accuracy. The multiple point boundary value problem was reformulated and a stable condensing algorithm was applied.

10. References

1. Speyer, J.L., "Nonoptimality of the Steady-State Cruise of Aircraft," AIAA Journal, Vol. 14, 1976, pp. 1604-1610.
2. Speyer, J.L., Dannemiller, D., Walker, D.,"Periodic Optimal Cruise of an Atmospheric Vehicle," Journal of Guidance, Control, and Dynamics, Vol. 8, 1985, pp. 31-38.
3. Gilbert, E.G., "Vehicle Cruise: Improved Fuel Economy by Periodic Control," Automatica, Vol. 12, 1976, pp. 159-166.
4. Breakwell, J.V., Shoee, H., "Minimum Fuel Flight Paths for Given Range," AIAA Paper, 1980, No. 80-1660.
5. Grimm, W., Well, K.-H., Oberle, H.J., "Periodic Control for Minimum Fuel Aircraft Trajectories", Journal of Guidance, Control, and Dynamics, Vol. 9, 1986, pp. 169-174.
6. Menon, P.K.A., "Study of Aircraft Cruise," Journal of Guidance, Control, and Dynamics, Vol. 12, 1989, pp. 631-639.
7. Sachs, G., "Verringerung des Treibstoffverbrauchs durch periodische Optimalflugbahnen," DGLR Jahrbuch, 1984, 090-1 - 09-17.
8. Sachs, G., Christodoulou, T., "Reducing Fuel Consumption of Subsonic Aircraft by Optimal Cyclic Cruise," Journal of Aircraft, Vol. 24, 1987, pp. 616-622.
9. Sachs, G., Lesch K., "Fuel Savings by Optimal Aircraft Cruise with Singular and Chattering Control," Lecture Notes in Control and Information Sciences, Springer-Verlag, (1990), pp. 590-599.
10. Sachs, G., Lesch K., "Optimal Periodic Cruise with Singular Control," AIAA Guidance, Navigation and Control Conference Proceedings, 1990, pp. 1586-1594.
11. ICAO Standard Atmosphere, International Civil Aviation Organization, Montreal, 1964.
12. Kumar, R., Kelley, H.J., "Singular Optimal Atmospheric Rocket Trajectories," Journal of Guidance, Control, and Dynamics, Vol. 11, 1988, pp. 305-312.
13. Bock , H.G., "Numerische Behandlung von Zustandsbeschränkten und Chebychef-Steuerungsproblemen," Course DR 3.10 of the Carl-Cranz-Gesellschaft, Oberpfaffenhofen, Germany, 1981.

14. Bock, H.G., "Randwertproblemmethoden zur Parameteridentifizierung in Systemen nichtlinearer Differentialgleichungen", Dissertation, Universität Bonn, 1985, Bonner Mathematische Schriften 183, Bonn, 1987.

15. ICAO Standard and Recommended Practices, Operation of Aircraft, Annex 6, 1986.

Author's Addresses

Prof. Dr.-Ing. Gottfried Sachs
Dipl.-Ing. Klaus Lesch

Institute of Flight Mechanics
and Flight Control
Technische Universität München
Arcisstr. 21
8000 München 2
Germany

Prof. Dr. Hans Georg Bock
Dipl.-Math. Marc Steinbach

Interdisciplinary Center
of Scientific Computing
Universität Heidelberg
Im Neuenheimer Feld 368
6900 Heidelberg
Germany

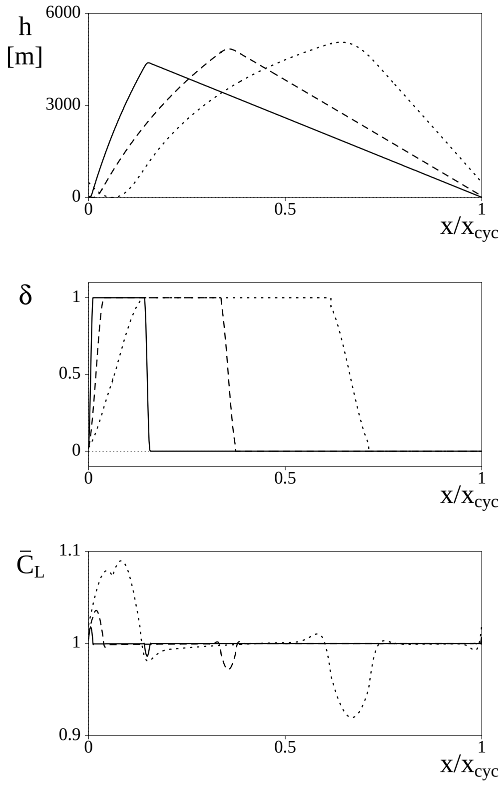

I ...... $E = 3.4$, $m/S = 345 \text{kg/m}^2$, $P_{\max}/(D_{\min}V_0^*) = 2.3$, $x_{\text{cyc}} = 51.4\,\text{km}$

II - - - - $E = 15$, $m/S = 214 \text{kg/m}^2$, $P_{\max}/(D_{\min}V_0^*) = 4.0$, $x_{\text{cyc}} = 116\,\text{km}$

III —— $E = 33$, $m/S = 45 \text{kg/m}^2$, $P_{\max}/(D_{\min}V_0^*) = 8.9$, $x_{\text{cyc}} = 174\,\text{km}$

Fig. 1 Optimal periods with singular arcs, altitude and control variables

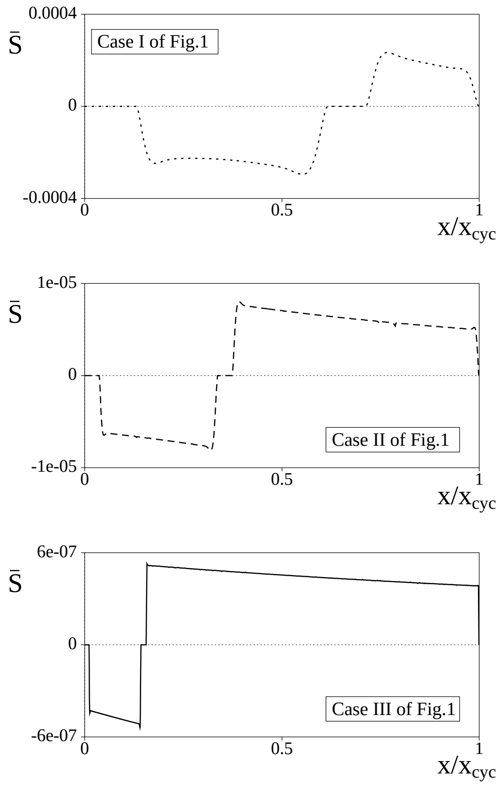

Fig. 2 Optimal periods with singular arcs, switching functions

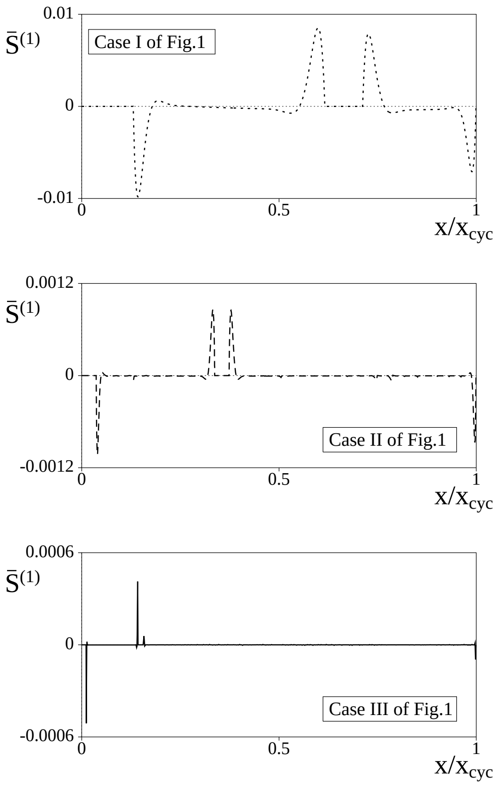

Fig. 3 Optimal periods with singular arcs, time derivatives of switching functions

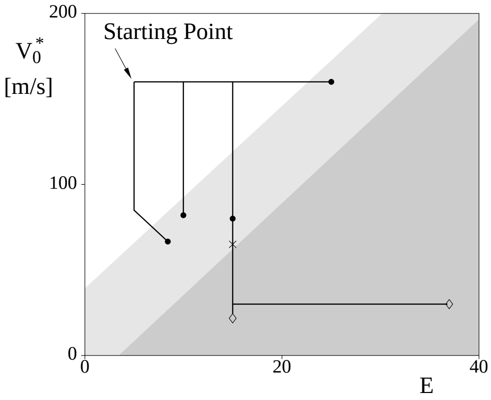

Fig. 4 Homotopy path

- ● Break down due to convergence failure, initial problem formulation
- × Break down due to convergence failure after normalization and time scaling
- ◇ Parameter values reached after numerical improvements

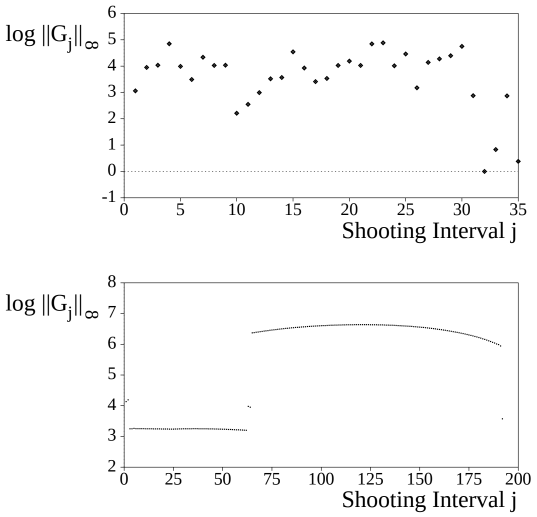

Fig. 5 Norms of transition matrices for solution at break-down point (32 intervals) and at end point of homotopy (192 intervals)
$E/(m/S) = 0.76\,\mathrm{kg/m^2}$, $C_{\mathrm{L}}^{*} = 0.78$

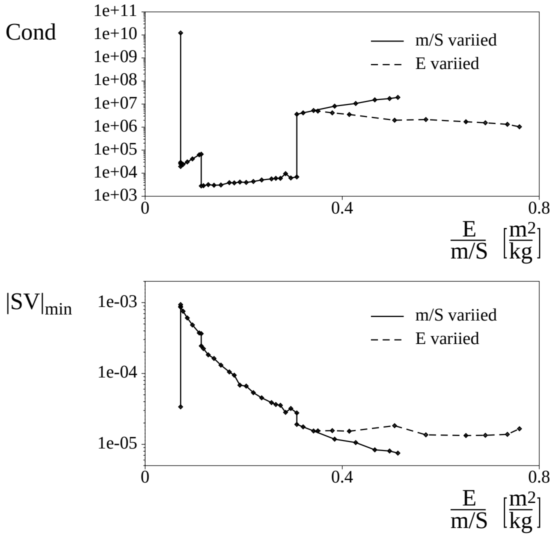

Fig. 6 Sub-condition numbers *Cond* of multipoint boundary conditions along homotopy branches and estimate of corresponding minimum singular values *SV*

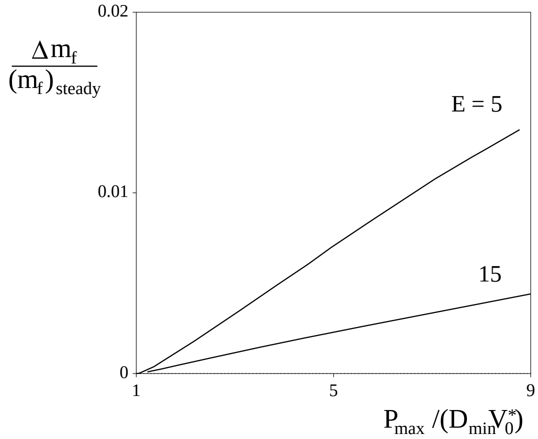

Fig. 7 Fuel saving Δm_f due to periodic optimal cruise with singular control
$(m_f)_{\mathrm{steady}}$: best steady-state cruise

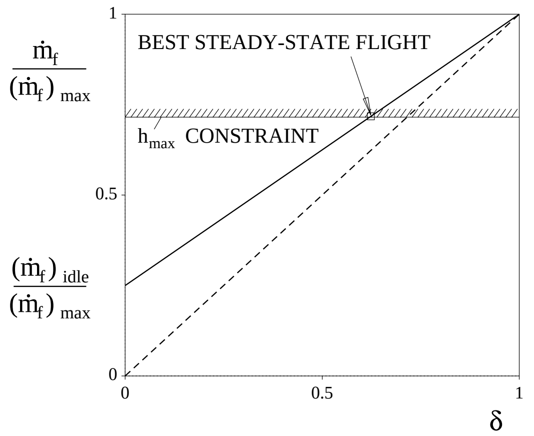

Fig. 8 Model with non-zero fuel consumption at idle thrust setting

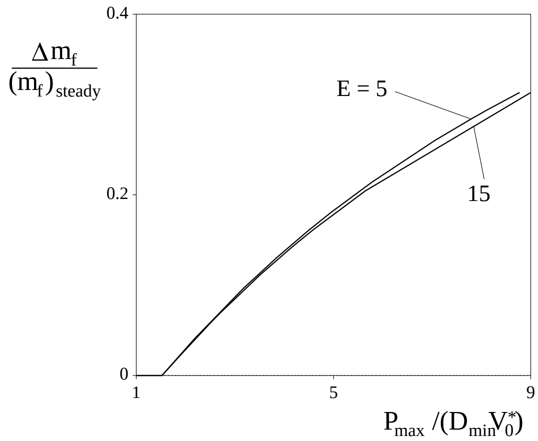

Fig. 9 Fuel saving Δm_f due to periodic optimal cruise
$(m_f)_{\mathrm{steady}}$: best steady-state cruise with a 3.5 km altitude limit $(\dot{m}_f)_{\mathrm{idle}}/(\dot{m}_f)_{\mathrm{max}} = 0.1$